JOC The Journal of Organic Chemistry

Article

Spiroconjugated Donor-#-Acceptor Charge-Transfer Dyes: E#ect of the #-Subsystems on the Optoelectronic Properties

Jan Wössner, and Birgit Esser

J. Org. Chem., **Just Accepted Manuscript** • DOI: 10.1021/acs.joc.0c00567 • Publication Date (Web): 17 Mar 2020

Just Accepted

is published by the American Chemical Society. 1155 Sixteenth Street N.W., Washington, DC 20036

Spiroconjugated Donor–σ–Acceptor Charge-Transfer Dyes: Effect of the π-Subsystems on the Optoelectronic Properties

Jan S. Wössner[†] and Birgit Esser*[,†,‡,§]

[†] Institute for Organic Chemistry, University of Freiburg, Albertstraße 21, 79104 Freiburg, Germany

[‡] Freiburg Materials Research Center, University of Freiburg, Stefan-Meier-Str. 21, 79104 Freiburg, Germany

[§] Cluster of Excellence livMatS @ FIT – Freiburg Center for Interactive Materials and Bioinspired Technologies, University of Freiburg, Georges-Köhler-Allee 105, 79110 Freiburg, Germany

ABSTRACT: Charge-transfer-based materials with intramolecular donor–acceptor structure are attractive for technological applications. Herein, a series of donor–σ–acceptor dyes has been prepared in a modular approach. The design of these intramolecular charge-transfer dyes is based on the concept of spiroconjugation, which leads to unique materials with special optical properties. The optical transitions are based on intramolecular charge-transfer, as shown by solvatochromic measurements and DFT-calculations. Crystallographic, computational, electrochemical and optical studies were performed to clarify the effect of different perpendicular π-moieties on the optoelectronic properties. Our molecular tuning allowed for the synthesis of molecules exhibiting strong visible-range absorption. The compounds are not fluorescent due to structural changes in the excited state, as revealed by DFT calculations. Finally, our study describes enantiomerically pure spiroconjugated absorber molecules using BINOL units on the donor part.

INTRODUCTION

In the past decades, solution-processable organic dyes have become important compounds based on their immense technological relevance for flexible, large-area and low-cost organic optoelectronic devices. Due to their charge-transfer properties, donor–acceptor (DA)-based compounds have been used as advanced organic materials for devices including solar cells, organic light-emitting diodes, electrochromic devices, and sensors.[1–6] Organic charge transfer molecules have been the primary focus as they provide better stability and flexibility in design than inorganic materials. Recent studies have illustrated that a twisting between donor and acceptor unit can lead to lower emission quantum yields as this structural change can enhance non-radiative deactivation processes.[7] Nevertheless, also non-emissive intramolecular charge-transfer dyes are relevant for applications, for example making use of nonlinear optical phenomena, which are based on the hyperpolarizability of the intramolecular charge transfer molecules.[8] The design of the DA compounds presented herein is based on the concept of spiroconjugation.[9,10] It is the through-space interaction between two mutually perpendicular π-subsystems, connected by a tetrahedral atom, which, in our case, is a carbon atom.[11,12] The two π-subsystems are a donor and acceptor moiety, as shown in Figure 1. If orbital symmetry permits, an interaction between orbitals of the subsystems is possible, as schematically depicted in Figure 1. Regarding an application in optical devices, an advantage of spirocompounds is their often non-crystalline, amorphous structure in the solid state. This prohibits the formation of π-π-aggregates and leads to stable morphologies. In the spiro-DA-compounds presented herein 1,3-indandione and derivatives thereof were used as acceptor units (Figure 1, right). These have been incorporated in the past by the groups of Schönberg,[13–16] Maslak,[17–20] Gleiter[21] and by us.[22] We recently reported on the syntheses and optical properties of spiroconjugated dyes, which contained 1,3-indandione-based acceptors with aromatic methylated diamines as donors.[23] In the spiro dyes presented herein the donors are aromatic amino thiols, aromatic thiols or aromatic alcohols (Figure 1, left). Combining those with 1,3-indandione-based acceptors led to fourteen spiro-DA-compounds. Herein, their syntheses, solid-state structures, optical and electrochemical properties are reported, supported by (TD)DFT calculations. Our studies suggest that such compounds are promising for solution-processable applications, and the unusual aromatic charge transfer based on spiroconjugation has great potential for constructing novel materials.

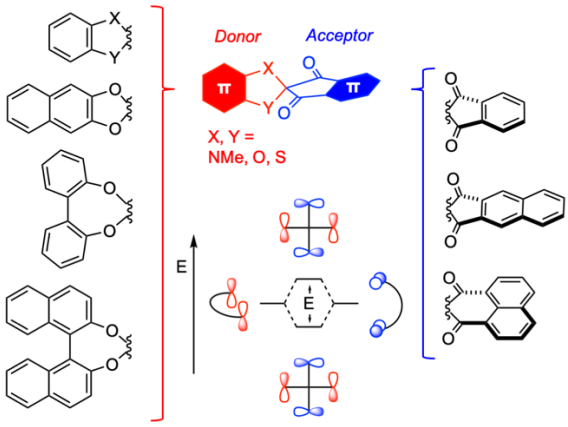

Figure 1. Donor-acceptor spiro compounds investigated herein and schematic energy diagram of the interaction between the two π-subsystems on either side of the spiro center.

RESULTS AND DISCUSSION

Synthesis and thermal stability. The syntheses of the spiro-DA-compounds are shown in Scheme 1 and Scheme 3. Basic hydrolysis of **1** led to the required 2-(methylamino)benzenethiol **2** in 93% yield. Subsequent condensation with benzo[*f*]ninhydrin (**3**)[23] under acid-catalysis and azeotropical removal of water furnished spiro-DA-compounds **4** in 71% yield. Under the same reaction conditions, condensation of benzene-1,2-dithiol (**5**) with ninhydrin (**6**) afforded S-CO-spiro compound **7** and its regioisomer **8** in 53% respective 28% yield, which could be separated by column chromatography.

Scheme 1. Synthesis of N/S-CO and S-CO-Spiro-DA Compounds 4, 7 and 8 by acid-catalyzed condensation.

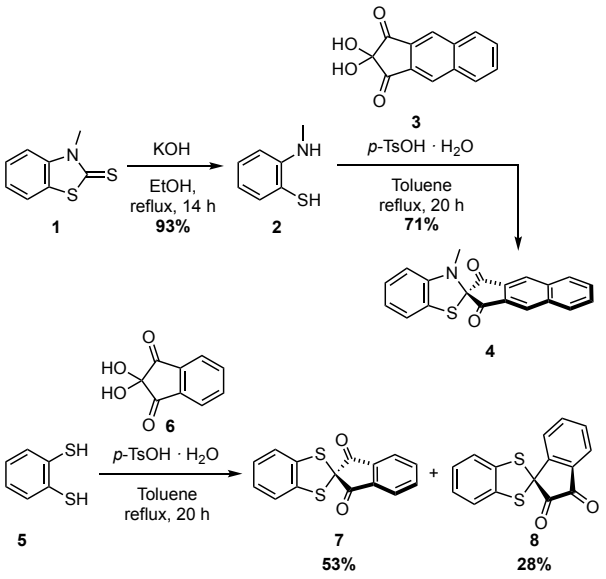

To avoid the formation of the regioisomer (corresponding to structure **8**) in the reaction with all other nucleophiles, we used dichloro-indandione derivatives instead of ninhydrin and its analogs as reaction partners. This allows for a condensation under basic conditions and successfully works for thiols or phenol derivatives as nucleophiles due to their relatively high acidity.

Scheme 2. Synthesis of 10 and 14.

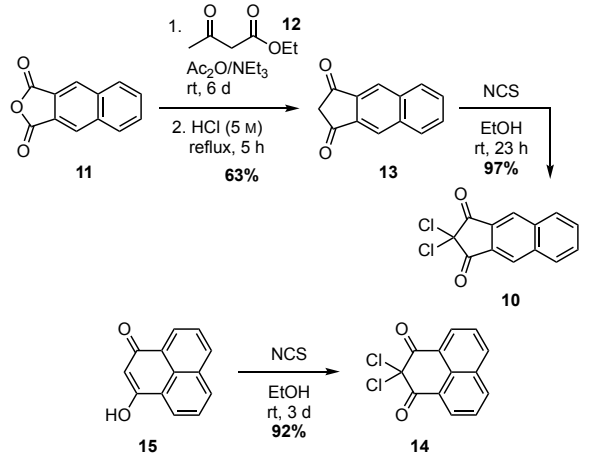

Dichloro-indandione (**9**) was synthesized according to the literature (Scheme 3).[24] Its benzannelated derivative **10** was accessed through condensation of naphtho[2,3-*c*]furan-1,3-dione (**11**) with ethyl 3-oxobutanoate (**12**) followed by strongly acidic hydrolysis and decarboxylation to furnish **13** (Scheme 2).[25] Double chlorination with *N*-chlorosuccinimide (NCS) afforded **10**. Naphthalene derivative **14** was accessed from 3-hydroxy-1*H*-phenalen-1-one (**15**) similarly by NCS chlorination. As nucleophiles we chose pyrocatechol (**16**), naphthalene-2,3-diol (**17**), [1,1'-biphenyl]-2,2'-diol (**18**), (*R*)-BINOL (**19**) and (S)-BINOL (**20**) (Scheme 3). Reaction of the three dichlorides **9**, **10** and **14** with these aromatic diols under basic conditions led to ten spiro-C-CO-compounds (Scheme 3). **21** and **22** have been reported before, however, were synthesized differently.[21] Furthermore, the S/O-CO-spiro compound **23** was synthesized by condensation of **9** with 2-mercaptophenol (**24**). BINOL-based spiro-compounds **28**, **29** and **32** are chiral and were synthesized in enantiomerically pure form.

The purity of the spiro compounds was confirmed by elemental analysis. Thermogravimetric analysis (TGA) and differential scanning calorimetry (DSC) provided information on the thermal properties of the 14 synthesized spiro compounds. The spiro compounds exhibited decomposition temperatures up to 348 °C (with 5% weight loss) as measured by thermal gravimetric analyses, demonstrating their excellent thermal stability (Figure S13–S14, SI). As shown in Figure S15 (SI), compound **7** displays obvious endothermic and exothermic peaks and 173 and 78 °C, respectively, in heating-cooling DSC cycles, which could be assigned to the corresponding melting and crystallization processes.

Crystallographic Studies. Single crystals suitable for X-ray diffraction were obtained for nine of the spiro-DA-compounds (Figure 2 and Supporting Information). These were grown by slow evaporation from $CDCl_3$ (**23**) or dichloromethane (**32**), by solvent layering from methanol/chloroform (**7**, **27**, **29**), dichloromethane/cyclohexane (**8**), chloroform/*n*-hexane (**21**) or chloroform/cyclohexane (**25**) or by vapor diffusion of DMSO/water at rt (**26**). The angle between the donor and acceptor part of the molecule was measured between the planes spanned by X–C_{spiro}–Y (where X, Y = S or O) and by (O)C–C_{spiro}–C(O). This angle amounted to 90.0° for **7**. The phenyl rings on the donor and acceptor part were slightly twisted away, resulting in an angle of 85.2°. In regioisomeric **8** these values amount to 90.0° and 89.9°, respectively, resulting in a perfectly perpendicular arrangement. In **23** and **21**, values of 87.1°/87.4° (**23**) and 89.8°/85.2° (**21**), were measured, while in **26** these amounted to 89.9°/89.8°. Due to the biphenyl units in **25** and **27**, the angle between the donor and acceptor aromatic systems deviated significantly from 90°. The dihedral angle between the phenyl groups in the biphenyl units amount to 36.9° for **25** and 40.8° for **27**. Figure 2b–e shows the packing of selected spiro-DA-compounds in the solid state. In **7** the nearest S-S-distances amount to 3.43 Å, indicating van-der-Waals bonding between these centers.[26] The perpendicular π-subsystems arranged themselves in opposite directions. **8**, on the other hand, exhibits dense molecular packing in a layered structure with closest S-S-contacts of 4.29 Å. In **23** the oxygen atom has relatively little impact on the solid-state structure, which is remarkably similar to that of compound **7** (see SI). Two neighboring molecules of **26** form a dimer in the crystal through slightly slipped face-to-face π–π stacking with an interplanar distance of about 3.5 Å. This π-stacking was not observed for the shorter aromatic system in **21**. In the structures containing a biphenol the packing becomes less ordered, and no packing symmetry is discernible due to the twisted structure of the two phenyl rings of the donor unit (Fig. S11, SI).

Scheme 3. Synthesis of 23 and O-CO-Spiro Compounds 21, 22, and 25–29.

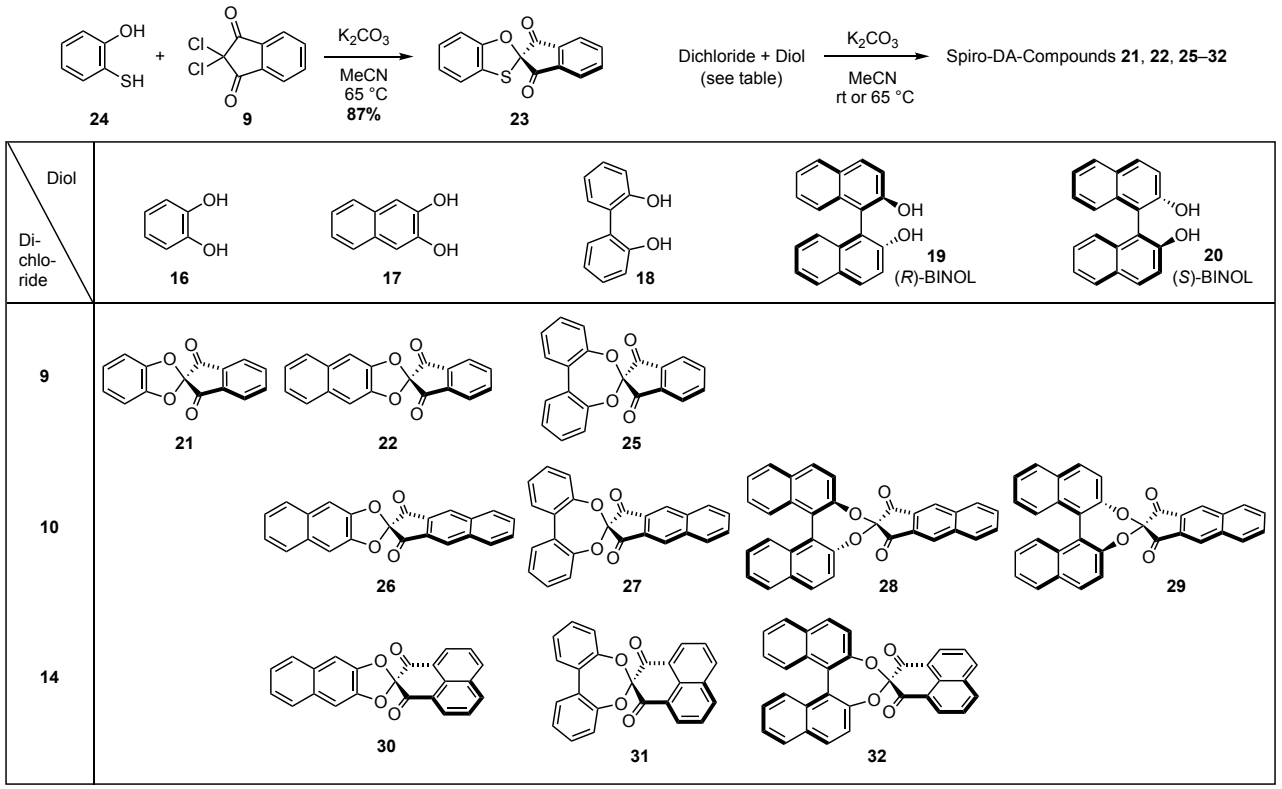

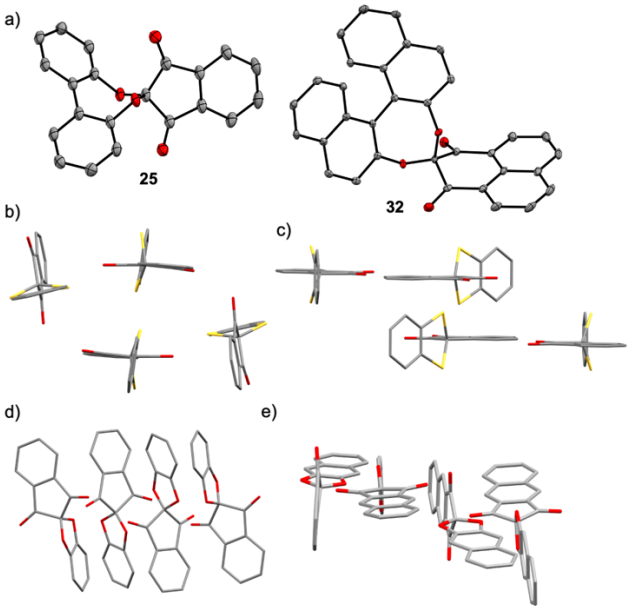

Figure 2: a) Molecular structures of selected spiro compounds in the solid-state (displacement ellipsoids are shown at 50% probability; hydrogen atoms are omitted for clarity). Molecular packing of b) **7**, c) **8**, d) **21**, and e) **26** in the solid-state.

Redox Properties. Figure 3 shows the cyclic voltammograms (CVs) of **4**, **7** and **8** in acetonitrile solution. All three molecules exhibited an irreversible oxidation (see also Table 1). The oxidation of **7** and **8** occurred at nearly the same anodic peak potential (1.09 V respective 1.12 V *vs.* Fc/Fc^+), since both contain the same dithio-donor moiety. The amino-thio-derivative **4**, in contrast, showed a significant shift to a lower peak potential of 0.55 V due to the presence of the nitrogen atom. As we have shown previously, replacing both sulfur atoms by nitrogen leads to a further lowering of the oxidation peak potential by ca. 0.5 V to 0.06 V *vs.* Fc/Fc^+.[23] The reduction potentials differed in all three spiro compounds. In **4** and **7**, containing a 1,3-(benz)indandione moiety, the reductions were irreversible and occurred at cathodic peak potentials of −1.45 and −1.26 V *vs.* Fc/Fc^+, respectively. The 1,2-indandione moiety in **8** allowed for a quasi-reversible reduction at an (in absolute values) higher half-wave potential of −1.07 V *vs.* Fc/Fc^+.

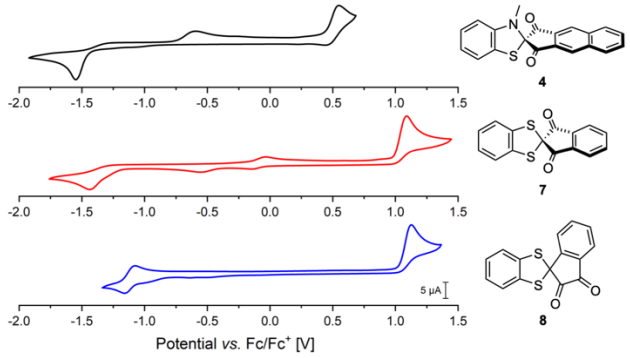

Figure 3: Cyclic voltammograms of **4**, **7**, and **8** (top to bottom; 1 mM in CH_3CN, 0.1 M n-Bu_4NPF_6, scan rate 0.1 mV s^{-1}, glassy carbon electrode).

Despite the high purity of all compounds, the CVs of **7** and **8** showed small peaks between −0.5 V and 0.0 V *vs.* Fc/Fc^+. These could have been caused by electrochemically induced side reactions, such as radical rearrangements of the formed species. When measured within a larger potential window, more than one reduction was observed for all three compounds (see SI).

Table 1. Electrochemical[a] and Optical Data[b] for Spiro Compounds 4, 7 and 8.

	E_{Red} [V][c]	E_{pa} [V][c]	E_{HOMO} [eV][d]	E_{LUMO} [eV][d]	λ_{CT} [nm][b]	$E_{g,opt}$ [eV][b,e]
4	−1.45 (E_{pc})	0.55	−5.23	−3.17	515	2.06
7	−1.26 (E_{pc})	1.09	−5.76	−3.09	405	2.67
8	−1.07 ($E_{1/2}$)	1.12	−5.83	−3.84	556	1.99

[a] 1 mM in CH_3CN, 0.1 M n-Bu_4NPF_6, scan rate 0.1 V s^{-1}, glassy carbon electrode; [b] in CH_2Cl_2; [c] *vs.* Fc/Fc^+; [d] from the onsets of the reduction/oxidation peaks, assuming an ionization energy of 4.8 eV for ferrocene;[27] [e] from the onsets of the longest wavelength absorption band.

Optical properties. The optical properties of all 14 spiro-DA-compounds were investigated by UV/Vis absorption spectroscopy (Figure 4a–d). All compounds displayed several absorption bands in the range of 300–700 nm. The lower wavelength bands at around 300–350 nm corresponded to π–π* transitions of the conjugated backbones, while the bands at higher wavelengths can be ascribed to intramolecular CT transitions. With the stronger N- or S-based donor units in **7**, **8**, **4** and **23**, the CT bands possessed higher intensities and/or appeared at higher wavelengths of 406, 556, 514, and 415 nm, respectively, compared to the O-based donors (Figure 4a). The *ortho*-quinone pattern in **8** led to a strong bathochromic shift of 150 nm compared to regioisomer **7**. The CT band of the smallest O-based DA-compound **21** occurred at a wavelength of 411 nm, similar to its S-congeners **7** (406 nm) and **23** (415 nm), but with much lower intensity (Figure 4b). Exchanging the donor unit from pyrocatechol in **21** to the biphenyl-diol in **25** hypsochromically shifted the CT band by 44 nm to 367 nm, likely due to the twist in the biphenyl unit decreasing conjugation in the donor unit. Extending the donor part in O-based **21** by benzo-fusion (**22**) led to a similar wavelength of the CT band of 414 nm (Figure 4b). Extending both the donor and acceptor unit as in **26** resulted in a bathochromic shift to 443 nm of the CT band (Figure 4c). Due to their structural similarity biphenol-based **27** and BINOL-based **28** have similar absorptions in the long wavelength region with two overlapping CT bands at 391 and 410 nm for **27** and at 392 and 412 nm for **28** (Figure 4c). The spectra of DA-compounds **32**, **31** and **30** with the phenalene-1,3-dione acceptor were markedly different. One to two broad and overlapping absorption bands are visible in Figure 4d between 300 and 350 nm.

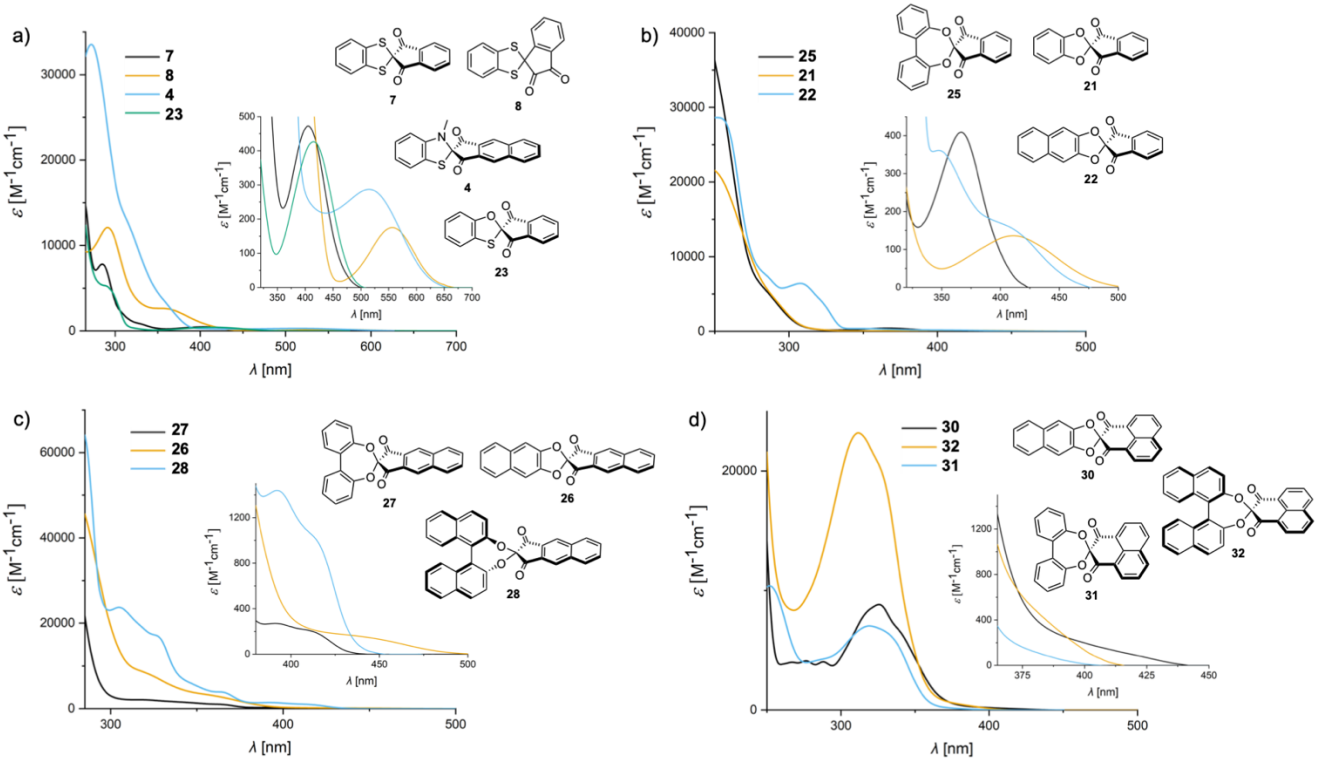

Figure 4. Absorption spectra of spiro-DA-compounds in CH_2Cl_2.

Figure 5 shows a comparison of the absorption spectrum of **22** with those of the naphthalene donor **33** and indane-1,3-dione acceptor part (**34**) as reference molecules. **33**[28] and **34**[23] were synthesized according to literature procedures. The DA compound **22** showed additional long-wavelength absorptions above 340 nm, which were absent for both reference molecules and stemmed from an intramolecular CT process.

4 was one of the spiro-DA-compounds demonstrating an expressed CT-band. This band showed pronounced negative solvatochromism and a hypsochromic shift occurred on increasing the solvent polarity (Figure 6).[23] This indicates that the ground state possessed a higher polarity than the first excited state. The CT band maximum shifted from 525 nm in toluene to 504 nm in acetonitrile. Compound **7** showed the same negative solvatochromic shift (Figure S12).

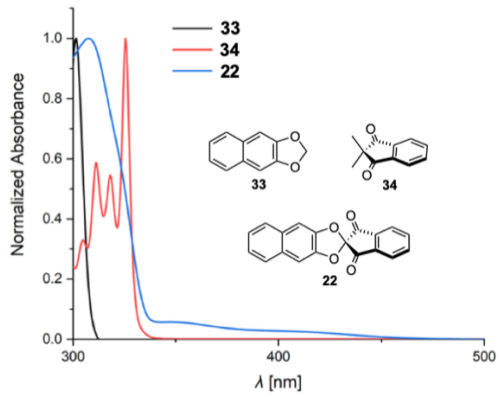

Figure 5. Absorption spectrum of spiro-DA-compound **22** in comparison to reference compounds **33** and **34** in CH_2Cl_2.

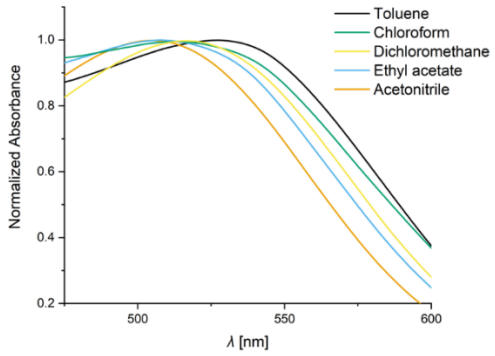

Figure 6. Absorption spectra of **4** measured in solvents of different polarity.

All spiro compounds investigated herein were non-fluorescent. Variations in the excitation wavelengths or changing solvent polarity ($CHCl_3$, CH_2Cl_2, toluene, *n*-hexane, methylcyclohexane) did not make a difference. Even degassed solutions of **4** to prevent quenching of a possibly involved triplet state by oxygen showed no emission.

Due to the incorporation of the enantiomerically pure BINOL donor units in **28** and **29**, these DA-spiro-compounds are chiral. The circular dichroic (CD) spectra of **28** and **29** displayed a mirror-image relationship and complementary Cotton effects of both the π-π*- and the CT transitions (Figure 7).

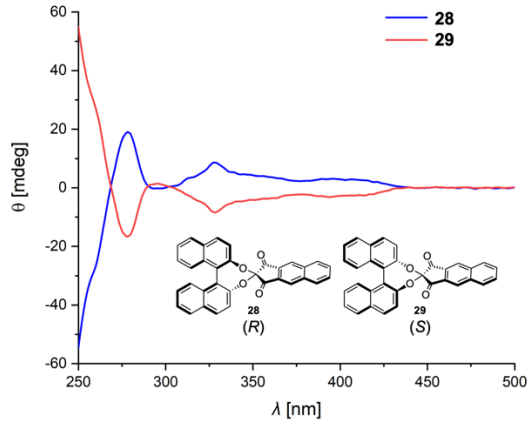

Figure 7. Circular dichroic (CD) spectra of BINOL-based **28** and **29** in CH_2Cl_2.

DFT calculations. Density functional theory (DFT) calculations were carried out at the B3LYP[29]-D3[30]/def2-TZVP[31] level using the Turbomole 7.3[32] package. In the frontier molecular orbitals for all spiro-DA-compounds, HOMO and LUMO are spatially well separated on the donor and acceptor part, respectively. In Figure 8, HOMO and LUMO of **7**, **8** and **26** are shown as examples. The electron density distribution of the LUMO is spread over the electron-poor β-diketone unit, while the HOMO is localized on the electronic-rich aromatic moiety. This is a good requirement for efficient charge separation in the excited state, demonstrated above through the CT bands in their UV/Vis absorption spectra.

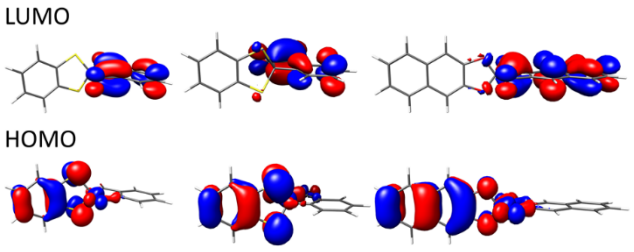

Figure 8. Calculated frontier molecular orbitals of **7**, **8** and **26** (B3LYP-D3/def2-TZVP).

The CT transition was further investigated for **4** on a theoretical level. DFT calculations showed that several CT transitions are possible increasing in energy from HOMO to LUMO, HOMO to LUMO+1 and HOMO−1 to LUMO (see Figure 9). The HOMO−1 to LUMO transition possesses the highest oscillator strength.

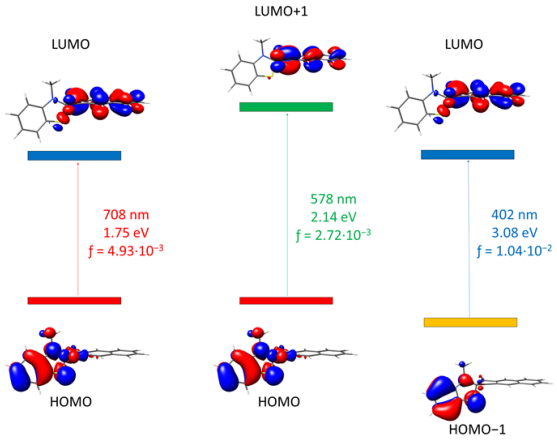

Figure 9. Calculated intramolecular charge-transfer transition of **4** (B3LYP-D3/def2-TZVP).

Upon excitation, **4** undergoes a geometrical rearrangement (Figure 10). The pyramidalization of the S and N-atom decreases in the S_1 compared to the S_0 state, resulting in a more symmetric arrangement of the acceptor relative to the donor part. The change in the molecular structure in the excited state implies a faster vibrational energy relaxation that explains the non-fluorescent nature of this the other spiro compounds. The excited vibrational modes of the spiro compounds are transferred to kinetic modes. The dynamic shape of the two lowest vibrational frequency modes (25.16 cm^{-1} and 28.36 cm^{-1}) clearly shows this nonradiative deactivation (supplementary animation 1–2).

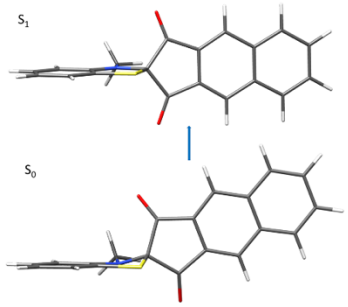

Figure 10. Optimized geometries of **4** in the ground (S_0) and first excited state (S_1) (PBEh-3c-D3/def2-mSVP).

CONCLUSIONS

We herein presented 14 donor-acceptor spiro derivatives using aromatic amino thiols, aromatic thiols or aromatic alcohols as donor units and 1,3-indandione-based acceptors, including two chiral, BINOL-based compounds. Their syntheses, electrochemical and optical properties were investigated, supported by DFT calculations. Many of these compounds showed charge-transfer absorptions in the visible range. Our study shows that these charge-transfer absorptions can be significantly tuned by changing the donor or acceptor part.

EXPERIMENTAL SECTION

Materials and Methods

Chemicals were purchased from Acros-Organics, Alfa-Aesar, ChemPur, Merck, Sigma Aldrich or TCI and used directly without further purification unless otherwise specified. Moisture- or oxygen-sensitive reactions were carried out in dried glassware - heated under vacuum - using standard Schlenk techniques in an anhydrous argon atmosphere (Argon 5.0 from Sauerstoffwerke Friedrichshafen). Anhydrous solvents (THF, toluene, CH_2Cl_2) were obtained from an M. Braun solvent purification system (MB-SPS-800) and stored over activated molecular sieves (3 Å) for several days. Cyclohexane for column chromatography was purchased in technical grade and purified by distillation under reduced pressure. Other solvents were purchased and used in analytical grade. Neutral Al_2O_3 (Brockmann Activity I) was purchased from Machery-Nagel and used directly without further activation. Thin-layer chromatography was carried out using silica gel-coated aluminum plates with a fluorescence indicator (Merck 60 F_{254}). The visualization of spots was achieved using UV light (λ_{max} = 254 nm and 366 nm) or a $KMnO_4$ staining solution (3.0 g $KMnO_4$, 20 g K_2CO_3, 5.0 mL (5.0%) NaOH, 300 mL H_2O). Column chromatography was carried out using silica gel 60 (grain size 40–63 µm) from Machery-Nagel. Some purifications were performed using a Reveleris X2 flash chromatography instrument by Grace.

^1H and $^{13}C\{^1H\}$ NMR spectra were recorded at 300 K using the following spectrometers: Bruker Avance III HD [300.1 MHz (^1H)], Bruker Avance II [400.1 MHz (^1H), 101.6 MHz (^{13}C)], Bruker Avance III HD [500.3 MHz (^1H), 125.8 MHz (^{13}C)]. Chemical shifts are reported in parts per million (ppm, δ = = scale) relative to the signal of tetramethylsilane (δ = 0.00 ppm). ^1H NMR spectra are referenced to tetramethylsilane as an internal standard or the residual solvent signal of the respective solvent: $CDCl_3$: δ = 7.26 ppm, CD_2Cl_2: δ = 5.32 ppm, DMSO-d_6: δ = 2.50 ppm. ^{13}C NMR spectra are referenced to the following signals: $CDCl_3$: δ = 77.16 ppm, CD_2Cl_2: δ = 54.00 ppm, DMSO-d_6: δ = 39.52 ppm. The following abbreviations for multiplicities were used: singlet (s), broad singlet (br), doublet (d), triplet (t), quartet (q), multiplet (m) and combinations thereof, i.e. doublet of doublets (dd). Coupling constants (J) are given in Hertz [Hz]. HRMS spectra were measured on a Thermo Fisher Scientific inc. Exactive or LCQ Advantage via electron spray ionization (ESI) or atmospheric pressure chemical ionization (APCI) with an orbitrap analyser. Ultraviolet/visible spectra were measured on a Tidas I diode array spectrometer (J&M Analytik) or a Perkin Elmer Lambda 950. Measurements were performed in a 10 mm quartz cuvette.

Cyclic voltammograms were measured in solution under an argon atmosphere using a Metrohm Autolab PGSTAT 128N. As working electrodes, a carbon paste or platinum electrode (2 mm diameter) was used. The spectra are referenced to the ferrocene/ferrocenium (Fc/Fc^+) redox couple. Single Crystal X-Ray Analysis was performed on a BRUKER APEX-II CCD diffractometer. A suitable crystal was selected and mounted on a MiTeGen holder in perfluoroether oil. For TGA an STA 409 by Netzsch and for DSC a Seiko 6200 by Seiko were used.

Synthetic Manipulations

2-(Methylamino)benzenethiol (2). To a solution of 3-methylbenzo[*d*]thiazole-2(3*H*)-thione (**1**, 2.03 mg, 11.2 mmol, 1.0 equiv.) in degassed EtOH (40 mL) was added KOH (8.12 g, 144 mmol, 12.9 equiv.) in one portion. The mixture was refluxed for 14 h under an argon atmosphere and then allowed to cool to rt. The reaction mixture was cooled to 0 °C, diluted by the addition of H_2O (300 mL) and treated with conc. aq. HCl until pH 7 was reached. The aqueous mixture was extracted with CH_2Cl_2 (5 × 40 mL). The organic extracts were dried over $MgSO_4$, filtered, and the solvent was removed *in vacuo*. Column chromatography (silica gel, cyclohexane/DCM: 1/0 to 1/1) afforded **2** (1.45 g, 93%) as a yellow crystalline solid. R_f = 0.83 (cyclohexane/EtOAc: 4/1); ^1H NMR (500 MHz, $CDCl_3$) δ = 7.30–7.22 (m, 1H), 7.20 (dd, J = 7.6, 1.7 Hz, 1H), 6.59 (dd, J = 8.2, 1.2 Hz, 1H), 6.56–6.51 (m, 1H), 4.90 (bs, 1H), 2.79 (s, 3H); ^{13}C NMR (126 MHz, $CDCl_3$) δ = 150.5, 137.1, 132.2, 118.6, 116.3, 109.9, 30.5; HRMS (APCI–): m/z calcd. for $C_7H_8SN^-$ 138.0383 $[M-H]^-$, found 138.0384.

3-Methyl-3*H*-spiro[benzo[*d*]thiazole-2,2'-cyclopenta[*b*]naphthalene]-1',3'-dione (4). A flame-dried flask was charged with 2-(methylamino)benzenethiol (**2**, 203 mg, 1.46 mmol, 1.0 equiv.), 2,2-dihydroxy-1*H*-cyclopenta[*b*]naphthalene-1,3(2*H*)-dione (**3**, 363 mg, 1.59 mmol, 1.1 equiv.), and *p*-TsOH · H_2O (5.47 mg, 28.7 µmol, 2 mol%). The flask was evacuated and backfilled with argon, and degassed anhydrous toluene (30 mL) was added. The reaction mixture was refluxed for 7 h, during which water was azeotropically removed using a *Dean-Stark*-type apparatus. The reaction was allowed to cool to rt and quenched by addition of sat. aq. $NaHCO_3$ (50 mL). The layers were separated, and the aqueous layer was extracted with CH_2Cl_2 (4 × 20 mL). The organic extracts were dried over $MgSO_4$, filtered, and the solvent was removed *in vacuo*. Column chromatography (silica gel, cyclohexane/CH_2Cl_2: 1/0 to 0/1) afforded **4** (343 mg, 71%) as a purple-red solid. R_f = 0.46 (cyclohexane/EtOAc: 4/1); ^1H NMR (500 MHz, $CDCl_3$) δ = 8.65 (s, 2H), 8.21–8.09 (m, 2H), 7.83–7.73 (m, 2H), 7.10 (ddd, J = 7.8, 7.8, 1.3 Hz, 1H), 6.95 (dd, J = 7.6, 1.2 Hz, 1H), 6.74 (ddd, J = 7.6, 7.5, 1.1 Hz, 1H), 6.47 (dd, J = 8.0, 1.0 Hz, 1H), 2.83 (s, 3H); ^{13}C NMR (126 MHz, $CDCl_3$) δ = 193.1, 147.8, 137.1, 134.8, 130.8, 130.5, 127.2, 126.3, 122.2, 121.3, 119.6, 107.6, 80.3, 32.1; HRMS (ESI+): m/z calcd. for $C_{20}H_{14}O_2NS^+$ 332.0740 $[M+H]^+$, found 332.0742; λ_{max} (log ε) = 515 (2.46).

Spiro[benzo[*d*][1,3]dithiole-2,2'-indene]-1',3'-dione (7) and spiro[benzo[*d*][1,3]dithiole-2,1'-indene]-2',3'-dione (8). A flame-dried flask was charged with benzene-1,2-dithiol (**5**, 250 mg, 1.76 mmol, 1.0 equiv.), 2,2-dihydroxy-1*H*-indene-1,3(2*H*)-dione (**6**, 344 mg, 1.93 mmol, 1.1 equiv.) and *p*-TsOH · H_2O (20.1 mg, 105 µmol, 6 mol%). The flask was evacuated and backfilled with argon and degassed anhydrous toluene (15 mL) was added. The reaction mixture was refluxed for 14 h, during which water was azeotropically removed using a *Dean-Stark*-type apparatus. The reaction was allowed to cool to rt and quenched by addition of sat. aq. $NaHCO_3$ (30 mL). The layers were separated, and the aqueous layer was extracted with CH_2Cl_2 (5 × 20 mL). The organic extracts were dried over $MgSO_4$, filtered, and the solvent was removed *in vacuo*. Column chromatography (silica gel, cyclohexane/EtOAc: 1/0 to 1/10) afforded **7** (263 mg, 53%) as a yellow solid and **8** (142 mg, 28%) as a dark green solid.

Analytical data for **7**: R_f = 0.22 (cyclohexane/EtOAc: 9/1); ^1H NMR (500 MHz, $CDCl_3$) δ = 8.14–8.06 (m, 2H), 8.00–7.89 (m, 2H), 7.20–7.14 (m, 2H), 7.14–7.07 (m, 2H); ^{13}C NMR (126 MHz, $CDCl_3$) δ = 191.8, 139.9, 137.2, 135.4, 126.9, 125.1, 122.1, 65.9; HRMS (APCI+): m/z calcd. for

$C_{15}H_9O_2S_2^+$ 285.0038 [M+H]$^+$, found 285.0037; elemental analysis calcd (%) for $C_{15}H_8O_2S_2$: C 63.36, H 2.84, S 22.55; found: C 63.24, H 2.81, S 24.34; λ_{max} (log ε) = 405 (2.67); mp = 169 °C.

Analytical data for **8**: R_f = 0.18 (cyclohexane/EtOAc: 9/1); ^{1}H NMR (500 MHz, CD_2Cl_2) δ = 8.38–8.35 (m, 1H), 7.93 (ddd, *J* = 7.9, 7.4, 1.2 Hz, 1H), 7.89 (ddd, *J* = 7.9, 1.2, 0.7 Hz, 1H), 7.69–7.62 (m, 1H), 7.17 (s, 4H); ^{13}C NMR (126 MHz, CD_2Cl_2) δ = 189.2, 188.0, 144.5, 139.0, 137.5, 136.7, 131.9, 128.6, 127.9, 124.6, 122.4, 62.1; HRMS (APCI+): *m*/*z* calcd. for $C_{15}H_9O_2S_2^+$ 285.0038 [M+H]$^+$, found 285.0035; elemental analysis calcd (%) for $C_{15}H_8O_2S_2$: C 63.36, H 2.84, S 22.55; found: C 63.11, H 2.83, S 24.23; λ_{max} (log ε) = 558 (2.46); mp = 176 °C.

1*H*-Cyclopenta[b]naphthalene-1,3(2*H*)-dione (13). Naphtho[2,3-*c*]furan-1,3-dione (**11**, 15.1 g, 76.2 mmol, 1.0 equiv.) was added to a solution of degassed anhydrous NEt_3 (60 mL) and degassed Ac_2O (80 mL). Degassed ethyl acetoacetate (**12**, 29.2 mL, 29.7 g, 228 mmol, 3.0 equiv.) was added dropwise. The reaction mixture was stirred at rt for 4 d under an argon atmosphere. The black solution was dissolved in H_2O (900 mL), and conc. HCl (200 mL) was added dropwise. The reaction mixture was stirred at rt for 30 min. A yellow precipitate formed, was filtered off and washed with H_2O (5 × 200 mL). The resulting yellow solid was suspended in aq. HCl (6 M, 200 mL), and the suspension was refluxed for 4 h and then allowed to cool to rt. A yellow precipitate was obtained and filtered off. Column chromatography (silica gel, cyclohexane/CH_2Cl_2 1/0 to 0/1) afforded **13** (9.43 g, 63%) as a pale-yellow solid. R_f = 0.17 (CH_2Cl_2); ^{1}H NMR (400 MHz, $CDCl_3$) δ = 8.57–7.44 (m, 2H), 2H), 8.17–8.04 (m, 2H), 7.79–7.68 (m, 2H), 3.37 (s, 2H); ^{13}C NMR (101 MHz, $CDCl_3$) δ = 197.7, 138.4, 136.5, 130.8, 129.8, 124.4, 46.9; HRMS (ESI+): *m*/*z* calcd. for $C_{13}H_9O_2^+$ 197.0597 [M+H]$^+$, found 197.0599.

2,2-Dichloro-1*H*-cyclopenta[*b*]naphthalene-1,3(2*H*)-dione (10). *N*-Chlorosuccinimide (2.65 g, 19.8 mmol, 2.2 equiv.) was added to a solution of 1*H*-cyclopenta[*b*]naphthalene-1,3(2*H*)-dione (**13**, 1.77 g, 9.02 mmol. 1.0 equiv.) in EtOH (20 mL). The reaction mixture was stirred at rt for 23 h. H_2O (60 mL) and EtOAc (20 mL) were added, and the reaction mixture was stirred for a further 5 min. The organic layer was separated, and the aqueous layer was extracted with EtOAc (4 × 30 mL). The combined organic layers were dried over $MgSO_4$, filtered, and the solvent was removed *in vacuo*. Column chromatography (silica gel, cyclohexane/CH_2Cl_2: 1/0 to 1/1) afforded **10** (2.31 g, 97%) as a colorless solid. R_f = 0.91 (CH_2Cl_2); ^{1}H NMR (400 MHz, $CDCl_3$) δ = 8.71–8.68 (m, 2H), 8.22–8.13 (m, 2H), 7.87–7.77 (m, 2H); ^{13}C NMR (101 MHz, $CDCl_3$) δ = 186.8, 137.6, 131.6, 131.1, 130.9, 127.9, 74.0; HRMS (ESI–): *m*/*z* calcd. for $C_{13}H_5Cl_2^-$ 262.9672 [M–H]$^-$, found 262.9672.

3-Hydroxy-1*H*-phenalen-1-one (15). 15 was synthesized using a modified literature procedure.[33] 1*H*,3*H*-Benzo[*de*]isochromene-1,3-dione (2.03 g, 10.2 mmol, 1.0 equiv.) was added to a suspension of anhydrous zinc chloride (4.18 g, 30.7 mmol, 30 equiv.) in degassed diethyl malonate (15.6 mL, 16.4 g, 102 mmol, 10 equiv.). The reaction mixture was stirred at 175 °C for 14 h. After cooling to rt, the mixture was diluted with CH_2Cl_2 (30 mL). The suspension was adsorbed on silica *in vacuo*. Column chromatography (silica gel, cyclohexane/EtOAc: 1/0 to 0/1) afforded **15** (1.84 g, 92%) as a yellow solid. R_f = 0.05 (cyclohexane/EtOAc: 4/1); ^{1}H NMR (500 MHz, DMSO-d_6) δ = 8.30 (dd, *J* = 7.2, 1.1 Hz, 2H), 8.26 (dd, *J* = 8.3, 1.1 Hz, 2H), 7.75 (dd, *J* = 8.3, 7.2 Hz, 2H), 6.03 (s, 1H); ^{13}C NMR (126 MHz, DMSO-d_6) δ = 178.3, 131.7, 131.5, 129.7, 127.4, 126.5, 126.1, 106.1; HRMS (ESI–): m/z calcd. for $C_{13}H_7O_2^-$ 195.0452 [M–H]$^-$, found 195.0451.

2,2-Dichloro-1*H*-phenalene-1,3(2*H*)-dione (14). *N*-Chlorosuccinimide (7.53 g, 56.4 mmol, 2.2 equiv.) was added to a suspension of 1*H*-phenalene-1,3(2*H*)-dione (**15**, 5.03 g, 25.6 mmol, 1.0 equiv.) in EtOH (100 mL). The reaction mixture was stirred at rt for 3 d. H_2O (300 mL) and EtOAc (100 mL) were added, and the reaction mixture was stirred for a further 5 min. The organic layer was separated, and the aqueous layer was extracted with EtOAc (5 × 80 mL). The combined organic layers were dried over $MgSO_4$, filtered, and the solvent was removed *in vacuo*. Column chromatography (silica gel, cyclohexane/EtOAc: 1/0 to 4/1) afforded **14** (6.23 g, 92%) as a white solid. R_f = 0.47 (cyclohexane/EtOAc:4/1); ^{1}H NMR (300 MHz, $CDCl_3$) δ = 8.59 (dd, *J* = 7.3, 1.2 Hz, 2H), 8.31 (dd, *J* = 8.3, 1.2 Hz, 2H), 7.82 (dd, *J* = 8.3, 7.3 Hz, 2H); ^{13}C NMR (101 MHz, $CDCl_3$) δ = 183.0, 135.9, 132.9, 131.9, 130.2, 127.26, 125.0, 83.8; HRMS (ESI+): *m*/*z* calcd. for $C_{13}H_7O_2{}^{37}Cl_2^+$ 268.9759 [M+H]$^+$, found 268.9756.

General procedure A for the synthesis of spiro compounds: A flame-dried flask was charged with 2,2-dichlorocompound, 1,2-diol and K_2CO_3. The flask was evacuated and backfilled with argon, and anhydrous acetonitrile (20 mL) was added. The reaction mixture was oil bath-heated to 65 °C in a sealed flask for 24 h. The reaction mixture was allowed to cool to rt and was poured into H_2O (200 mL). The aqueous reaction mixture was extracted with CH_2Cl_2 (5 × 25 mL). The organic extracts were dried over $MgSO_4$, filtered, and the solvent was removed *in vacuo.*

General procedure B for the synthesis of spiro compounds: A flame-dried flask was charged with 2,2-dichlorocompound, 1,2-diol and K_2CO_3. The flask was evacuated and backfilled with argon, and anhydrous acetonitrile (20 mL) was added. The reaction mixture was stirred at rt in a sealed flask for 24 h. The reaction mixture was allowed to cool to rt and was poured into H_2O (200 mL). The aqueous reaction mixture was extracted with CH_2Cl_2 (5 × 25 mL). The organic extracts were dried over $MgSO_4$, filtered, and the solvent was removed *in vacuo*.

Spiro[benzo[*d*][1,3]dioxole-2,2'-indene]-1',3'-dione (21). 21 was synthesized following the general procedure A using 2,2-dichloro-1*H*-indene-1,3(2*H*)-dione (**9**, 534mg, 2.48 mmol, 1.0 equiv.), benzene-1,2-diol (**16**, 328 mg, 2.98 mmol, 1.2 equiv.) and K_2CO_3 (1.75 g, 12.7 mmol, 5.1 equiv.). Column chromatography (silica gel, cyclohexane/CH_2Cl_2: 1/0 to 1/1) afforded **21** (484 mg, 77%) as a yellow solid. R_f = 0.21 (cyclohexane/CH_2Cl_2: 3/2); ^{1}H NMR (400 MHz, $CDCl_3$) δ = 8.18–8.06 (m, 2H), 8.06–7.92 (m, 2H), 6.99–6.82 (m, 4H); ^{13}C NMR (101 MHz, $CDCl_3$) δ = 189.8, 147.2, 140.5, 137.7, 124.9, 122.7, 109.0, 100.3; HRMS (APCI+): *m*/*z* calcd. for $C_{15}H_{12}O_4N^+$ 270.0761 [M+NH_4]$^+$, found 270.0757; elemental analysis calcd (%) for $C_{15}H_8O_4$: C 71.43, H 3.20; found: C 71.21, H 3.25; UV/Vis (CH_2Cl_2): λ_{max} (log ε) = 412 (2.13); mp = 167 °C.

Spiro[indene-2,2'-naphtho[2,3-*d*][1,3]dioxole]-1,3-dione (22). 22 was synthesized following the general procedure A using 2,2-dichloro-1*H*-indene-1,3(2*H*)-dione (**9**, 486 mg, 2.26 mmol, 1.0 equiv.), naphthalene-2,3-diol (**17**, 471 mg, 2.94 mmol, 1.3 equiv.) and K_2CO_3 (1.25 g, 9.04 mmol, 4.0 equiv.). Column chromatography (silica gel, cyclohexane/CH_2Cl_2: 1/0 to 1/1) afforded **22** (607 mg, 89%) as a yellow solid. R_f = 0.20 (cyclohexane/CH_2Cl_2: 1/1); ^{1}H NMR (400 MHz, $CDCl_3$) δ = 8.18–8.12 (m, 2H), 8.05–7.99 (m, 2H), 7.73–7.67 (m, 2H), 7.40–7.33 (m, 2H), 7.24–7.21 (m, 2H), ^{13}C NMR (101 MHz, $CDCl_3$) δ = 189.6, 147.3, 140.5, 137.8, 130.8, 127.5, 125.1, 125.0, 104.7, 100.3; HRMS (ESI+): *m*/*z* calcd. for $C_{19}H_{10}O_4$ 302.0574 [M]$^+$, found 302.0574; elemental analysis calcd (%) for $C_{19}H_{10}O_4$: C 75.49, H 3.33; found: C 75.31, H, 3.36; UV/Vis (CH_2Cl_2): λ_{max} (log ε) = 348 (2.55); mp = 188 °C.

Spiro[benzo[*d*][1,3]oxathiole-2,2'-indene]-1',3'-dione (23). 23 was synthesized following the general procedure A using 2,2-dichloro-1*H*-indene-1,3(2*H*)-dione (**9**, 523 mg, 2.43 mmol, 1.0 equiv.), 2-mercaptophenol (**24**, 471 mg, 2.94 mmol, 1.3 equiv.) and K_2CO_3 (1.68 g, 12.2 mmol, 5.0 equiv.). Column chromatography (silica gel, cyclohexane/CH_2Cl_2: 1/0 to 1/1) afforded **23** (567 mg, 87%) as a yellow solid. R_f = 0.81 (CH_2Cl_2); ^{1}H NMR (400 MHz, $CDCl_3$) δ = 8.16–8.04 (m, 2H), 8.04–7.92 (m, 2H), 7.17–7.06 (m, 2H), 7.05–6.88 (m, 2H); ^{13}C NMR (101 MHz, $CDCl_3$) δ = 190.2, 156.0, 139.6, 137.4, 127.4, 125.1, 123.6, 121.7, 111.0, 89.0; HRMS (ESI+): *m*/*z* calcd. for $C_{15}H_9O_3S^+$ 269.0267 [M+H]$^+$, found 269.0267; elemental analysis calcd (%) for $C_{15}H_8O_3S$: C 67.15, H 3.01, S 11.95; found: C 67.34, H 3.00, S 12.88; UV/Vis (CH_2Cl_2): λ_{max} (log ε) = 415 (2.62); mp = 159 °C.

Spiro[dibenzo[*d*,*f*][1,3]dioxepine-6,2'-indene]-1',3'-dione (25). 25 was synthesized following the general procedure A using 2,2-dichloro-1*H*-indene-1,3(2*H*)-dione (**9**, 612 mg, 2.85 mmol, 1.0 equiv.), [1,1'-biphenyl]-2,2'-diol (**18**, 471 mg, 2.94 mmol, 1.3 equiv.) and K_2CO_3 (5.10 g, 14.5 mmol, 4.0 equiv.). Column chromatography (silica gel, cyclohexane/CH_2Cl_2: 1/0 to 1/1) afforded **25** (647 mg, 69%) as a pale yellow solid. R_f = 0.47 (cyclohexane/CH_2Cl_2: 1/1); ^{1}H NMR (500 MHz, $CDCl_3$) δ = 8.14–7.06 (m, 2H), 8.00–7.93 (m, 2H), 7.59–7.54 (m, 2H), 7.41–7.35 (m, 4H), 7.16–7.09 (m, 2H); ^{13}C NMR (126 MHz, $CDCl_3$) δ = 190.9, 150.7,

139.4, 137.3, 131.5, 129.2, 128.8, 126.5, 124.7, 122.8, 101.5; HRMS (ESI+): m/z calcd. for $C_{21}H_{13}O_4^+$ 329.0808 $[M+H]^+$, found 329.0806; elemental analysis calcd (%) for $C_{21}H_{12}O_4$: C 76.82, H 3.68; found: C 76.94, H 3.80; UV/Vis (CH_2Cl_2): λ_{max} (log ε) = 367 (2.61), ; mp = 178 °C.

Spiro[cyclopenta[*b*]naphthalene-2,2'-naphtho[2,3-*d*][1,3]dioxole]-1,3-dione (26). 26 was synthesized following the general procedure A using 2,2-dichloro-1*H*-cyclopenta[*b*]naphthalene-1,3(2*H*)-dione (**10**, 300 mg, 1.13 mmol, 1.0 equiv.), naphthalene-2,3-diol (**17**, 254 mg, 1.58 mmol, 1.4 equiv.) and K_2CO_3 (626 mg, 4.52 mmol, 4.0 equiv.). Column chromatography (silica gel, cyclohexane/CH_2Cl_2: 1/0 to 0/1) afforded **26** (343 mg, 86%) as a yellow solid. R_f = 0.81 (CH_2Cl_2); ^{1}H NMR (400 MHz, $CDCl_3$) δ = 8.76–8.71 (m, 2H), 8.24–8.16 (m, 2H), 7.88–7.80 (m, 2H), 7.75–7.67 (m, 2H), 7.42–7.33 (m, 2H), 7.24 (s, 2H); ^{13}C NMR (101 MHz, $CDCl_3$) δ = 190.0, 147.4, 137.4, 134.6, 131.1, 131.0, 130.9, 127.5, 126.8, 125.0, 104.7 (due to low solubility of this compounds, the spiro-C-atom is not visible); HRMS (APCI+): m/z calcd. for $C_{23}H_{13}O_4^+$ 353.0808 $[M+H]^+$, found 353.0808; elemental analysis calcd (%) for $C_{23}H_{12}O_4$: C 78.40, H 3.43; found: C 76.91, H 4.14; UV/Vis (CH_2Cl_2): λ_{max} (log ε) = 436 (2.20), ; mp = 293 °C.

Spiro[cyclopenta[b]naphthalene-2,6'-dibenzo[*d,f*][1,3]dioxepine]-1,3-dione (27). 27 was synthesized following the general procedure A using 2,2-dichloro-1*H*-cyclopenta[*b*]naphthalene-1,3(2*H*)-dione (**10**, 300 mg, 1.13 mmol, 1.0 equiv.), [1,1'-biphenyl]-2,2'-diol (**18**, 295 mg, 1.58 mmol, 1.4 equiv.) and K_2CO_3 (626 mg, 4.52 mmol, 4.0 equiv.) Column chromatography (silica gel, cyclohexane/CH_2Cl_2: 1/0 to 0/1) afforded **27** (312 mg, 73%) as a yellow solid. R_f = 0.81 (CH_2Cl_2); ^{1}H NMR (500 MHz, $CDCl_3$) δ = 8.67 (s, 2H), 8.20–8.14 (m, 2H), 7.83–7.77 (m, 2H), 7.61–7.55 (m, 2H), 7.43–7.36 (m, 4H), 7.18–7.12 (m, 2H); ^{13}C NMR (126 MHz, $CDCl_3$) δ = 191.1, 150.8, 137.3, 134.0, 131.6, 130.9, 130.5, 129.3, 128.9, 126.5, 126.4, 122.9, 102.1; HRMS (APCI+): m/z calcd. for $C_{25}H_{15}O_4^+$ 379.0965 $[M+H]^+$, found 379.0966; elemental analysis calcd (%) for $C_{25}H_{14}O_4$: C 79.36, H 3.73; found: C 79.61, H 3.81; UV/Vis (CH_2Cl_2): λ_{max} (log ε) = 392 (2.43), ; mp = 253 °C.

***(R)*-Spiro[cyclopenta[*b*]naphthalene-2,4'-dinaphtho[2,1-*d*:1',2'-*f*][1,3]dioxepine]-1,3-dione (28). 28** was synthesized following the general procedure B using 2,2-dichloro-1*H*-cyclopenta[*b*]naphthalene-1,3(2*H*)-dione (**10**, 309 mg, 1.17 mmol, 1.0 equiv.), (*R*)-[1,1′-binaphthalene]-2,2′-diol (**19**, 404 mg, 1.41 mmol, 1.2 equiv.) and K_2CO_3 (649 mg, 4.70 mmol, 4.0 equiv.). Column chromatography (silica gel, cyclohexane/CH_2Cl_2: 1/0 to 1/1) afforded **28** (468 mg, 83%) as a yellow crystalline solid. R_f = 0.49 (cyclohexane/CH_2Cl_2: 1/1); ^{1}H NMR (500 MHz, $CDCl_3$) δ = 8.66 (s, 2H), 8.19–8.13 (m, 2H), 8.02–7.99 (m, 2H), 7.99–7.96 (m, 2H), 7.80–7.75 (m, 2H), 7.53–7.50 (m, 2H), 7.49 (ddd, J = 8.1, 6.8, 1.2 Hz, 2H), 7.41 (d, J = 8.7 Hz, 2H), 7.32 (ddd, J = 8.4, 6.8, 1.2 Hz, 2H); ^{13}C NMR (126 MHz, $CDCl_3$) δ = 191.1, 149.0, 137.3, 134.0, 132.4, 132.3, 130.9, 130.6, 129.9, 128.6, 127.5, 126.4, 126.1, 125.5, 124.6, 122.4, 103.1; HRMS (APCI+): m/z calcd. for $C_{33}H_{19}O_4^+$ 479.1278 $[M+H]^+$, found 479.1281; elemental analysis calcd (%) for $C_{33}H_{18}O_4$: C 82.83, H 3.79; found: C 82.88, H 3.81; UV/Vis (CH_2Cl_2): λ_{max} (log ε) = 392 (3.16); mp = 287 °C.

***(S)*-Spiro[cyclopenta[*b*]naphthalene-2,4'-dinaphtho[2,1-*d*:1',2'-*f*][1,3]dioxepine]-1,3-dione (29). 29** was synthesized following the general procedure B using 2,2-dichloro-1*H*-cyclopenta[*b*]naphthalene-1,3(2*H*)-dione (**10**, 458 mg, 1.74 mmol, 1.0 equiv.), (*S*)-[1,1′-binaphthalene]-2,2′-diol (**20**, 598 mg, 2.09 mmol, 1.2 equiv.) and K_2CO_3 (962 mg, 6.96 mmol, 4.0 equiv. Column chromatography (silica gel, cyclohexane/CH_2Cl_2: 1/0 to 1/1) afforded **29** (707 mg, 85%) as a yellow crystalline solid. R_f = 0.49 (cyclohexane/CH_2Cl_2: 1/1); ^{1}H NMR (500 MHz, $CDCl_3$) δ = 8.66 (s, 2H), 8.21–8.13 (m, 2H), 8.01–7.99 (m, 2H), 7.99–7.96 (m, 2H), 7.82–7.75 (m, 2H), 7.53–7.50 (m, 2H), 7.49 (ddd, J = 8.1, 6.8, 1.2 Hz, 2H), 7.41 (d, J = 8.7 Hz, 2H), 7.31 (ddd, J = 8.4, 6.8, 1.2 Hz, 2H); ^{13}C NMR (126 MHz, $CDCl_3$) δ = 191.1, 149.0, 137.3, 134.0, 132.5, 132.3, 130.9, 130.6, 129.9, 128.6, 127.5, 126.4, 126.1, 125.5, 124.6, 122.4, 103.1; HRMS (APCI+): m/z calcd. for $C_{33}H_{19}O_4^+$ 479.1278 $[M+H]^+$, found 479.1281; elemental analysis calcd (%) for $C_{33}H_{18}O_4$: C 82.83, H 3.79; found: C 82.89, H 3.83; UV/Vis (CH_2Cl_2): λ_{max} (log ε) = 392 (3.16); mp = 287 °C.

1'*H*,3'*H*-Spiro[naphtho[2,3-*d*][1,3]dioxole-2,2'-phenalene]-1',3'-dione (30). 30 was synthesized following the general procedure A using 2,2-dichloro-1*H*-phenalene-1,3(2*H*)-dione (**14**, 501 mg, 1.89 mmol, 1.0 equiv.), naphthalene-2,3-diol (**17**, 363 mg, 2.26 mmol, 1.2 equiv.) and K_2CO_3 (1.05 g, 7.56 mmol, 4.0 equiv.). Column chromatography (silica gel, cyclohexane/CH_2Cl_2: 1/0 to 0/1) afforded **30** (507 mg, 82%) as a white solid. R_f = 0.73 (CH_2Cl_2); ^{1}H NMR (500 MHz, $CDCl_3$) δ = 8.55 (dd, J = 7.2, 1.3 Hz, 2H), 8.34 (dd, J = 8.3, 1.2 Hz, 2H), 7.82 (dd, J = 8.3, 7.2 Hz, 2H), 7.70–7.65 (m, 2H), 7.37–7.32 (m, 2H), 7.22 (s, 2H); ^{13}C NMR (126 MHz, $CDCl_3$) δ = 186.8, 146.9, 136.0, 133.3, 132.1, 130.7, 130.6, 127.5, 127.2, 127.1, 125.0, 105.6, 104.9; HRMS (ESI+): m/z calcd. for $C_{23}H_{13}O_4^+$ 353.0808 $[M+H]^+$, found 353.0807; elemental analysis calcd (%) for $C_{23}H_{12}O_4$: C 78.40, H 3.43; found: C 76.98, H 3.32; UV/Vis (CH_2Cl_2): λ_{max} (log ε) = 326 (3.95), ; mp = 319 °C.

1'H,3'H-Spiro[dibenzo[*d,f*][1,3]dioxepine-6,2'-phenalene]-1',3'-dione (31). 31 was synthesized following the general procedure A using 2,2-dichloro-1*H*-phenalene-1,3(2*H*)-dione (**14**, 261 mg, 0.98 mmol, 1.0 equiv.), [1,1'-biphenyl]-2,2'-diol (**18**, 220 mg, 1.18 mmol, 1.2 equiv.) and K_2CO_3 (544 mg, 3.94 mmol, 4.0 equiv.). Column chromatography (silica gel, cyclohexane/CH_2Cl_2: 1/0 to 1/1) afforded **31** (239 mg, 64%) as a white solid. R_f = 0.56 (cyclohexane/CH_2Cl_2: 1/1); ^{1}H NMR (400 MHz, CD_2Cl_2) δ = 8.45–8.39 (m, 2H), 8.37–8.30 (m, 2H), 7.88–7.77 (m, 2H), 7.60–7.50 (m, 2H), 7.42–7.30 (m, 4H), 7.18–7.05 (m, 2H); ^{13}C NMR (101 MHz, CD_2Cl_2) δ = 189.5, 151.9, 135.6, 133.6, 132.1, 131.8, 129.9, 129.7, 129.2, 128.8, 127.5, 126.7, 123.6, 110.2; HRMS (ESI+): m/z calcd. for $C_{25}H_{15}O_4$ 379.0965 $[M+H]^+$, found 379.0964; elemental analysis calcd (%) for $C_{25}H_{14}O_4$: C 78.96, H 3.83; found: C 78.28, H 3.77; UV/Vis (CH_2Cl_2): λ_{max} (log ε) = 319 (3.84); mp = 275 °C.

***(R)*-1'H,3'H-Spiro[dinaphtho[2,1-*d*:1',2'-*f*][1,3]dioxepine-4,2'-phenalene]-1',3'-dione (32). 32** was synthesized following the general procedure B using 2,2-dichloro-1*H*-phenalene-1,3(2*H*)-dione (**14**, 210 mg, 0.79 mmol, 1.0 equiv.), (*R*)-[1,1′-binaphthalene]-2,2′-diol (**19**, 272 mg, 0.95 mmol, 1.2 equiv.) and K_2CO_3 (438 mg, 3.17 mmol, 4.0 equiv.). Column chromatography (silica gel, cyclohexane/EtOAc: 1/0 to 1/1) afforded **32** (353 mg, 93%) as a white solid. R_f = 0.64 (cyclohexane/CH_2Cl_2: 1/1); ^{1}H NMR (500 MHz, CD_2Cl_2) δ = 8.39 (dd, J = 7.2, 1.2 Hz, 2H), 8.36 (dd, J = 8.4, 1.2 Hz, 2H), 7.99–7.93 (m, 4H), 7.84 (dd, J = 8.2, 7.2 Hz, 2H), 7.48 (ddd, J = 8.1, 6.7, 1.2 Hz, 2H), 7.43–7.36 (m, 4H), 7.29 (ddd, J = 8.5, 6.6, 1.3 Hz, 2H); ^{13}C NMR (126 MHz, CD_2Cl_2) δ = 189.5, 150.2, 135.6, 133.6, 132.5, 132.5, 131.8, 130.3, 129.9, 128.9, 128.8, 127.5, 127.5, 126.7, 126.0, 125.0, 123.0, 111.5; HRMS (ESI+): m/z calcd. for $C_{33}H_{22}O_4N^+$ 496.1543 $[M+NH_4]^+$, found 496.1541; elemental analysis calcd (%) for $C_{33}H_{18}O_4$: C 82.83, H 3.79; found: C 82.89, H 3.83; UV/Vis (CH_2Cl_2): λ_{max} (log ε) = 312 (4.36); ; mp = 264 °C.

ASSOCIATED CONTENT

Supporting Information

CCDC 1859605 (**7**), 1874678 (**8**), 1964046 (**13**), 1964067 (**14**), 1864464 (**21**), 1874255 (**23**), 1864468 (**25**), 1912192 (**26**), 1900045 (**27**), 1964127 (**29**), 1886536 (**32**) contain the supplementary crystallographic data for this paper. These data can be obtained free of charge from The Cambridge Crystallographic Data Centre via www.ccdc.cam.ac.uk/structures. The Supporting Information contains NMR spectra, X-ray crystallographic data, TGA and DSC measurements, further cyclic voltammograms, further computational results, and energies and Cartesian coordinates of calculated structures. The Supporting Information is available free of charge on the ACS Publications website.

AUTHOR INFORMATION

Corresponding Author

* besser@oc.uni-freiburg.de.

ORCID

Jan Wössner: 0000-0003-2170-4798

Birgit Esser: 0000-0002-2430-1380

Notes

The authors declare no competing financial interest.

ACKNOWLEDGMENT

J.W. thanks Martin Betschart for measurement of the CD spectra. Generous support by the German Research Foundation (ES 361/2-1, INST 40/467-1 FUGG) and the state of Baden-Württemberg through bwHPC is gratefully acknowledged.

REFERENCES

(1) Sasaki, S.; Drummen, G. P. C.; Konishi, G. Recent Advances in Twisted Intramolecular Charge Transfer (TICT) Fluorescence and Related Phenomena in Materials Chemistry. *J. Mater. Chem. C* **2016**, *4* (14), 2731–2743. https://doi.org/10.1039/C5TC03933A.

(2) Soto, J.; Imbarack, E.; López-Tocón, I.; Sánchez-Cortés, S.; Otero, J. C.; Leyton, P. Application of Surface-Enhanced Resonance Raman Scattering (SERS) to the Study of Organic Functional Materials: Electronic Structure and Charge Transfer Properties of 9,10-Bis((E)-2-(Pyridin-4-Yl)Vinyl)Anthracene. *RSC Adv.* **2019**, *9* (25), 14511–14519. https://doi.org/10.1039/C9RA01269A.

(3) Zheng, Z.; Awartani, O. M.; Gautam, B.; Liu, D.; Qin, Y.; Li, W.; Bataller, A.; Gundogdu, K.; Ade, H.; Hou, J. Efficient Charge Transfer and Fine-Tuned Energy Level Alignment in a THF-Processed Fullerene-Free Organic Solar Cell with 11.3% Efficiency. *Adv. Mater.* **2017**, *29* (5), 1604241. https://doi.org/10.1002/adma.201604241.

(4) Dong, Y.; Zhang, J.; Tan, X.; Wang, L.; Chen, J.; Li, B.; Ye, L.; Xu, B.; Zou, B.; Tian, W. Multi-Stimuli Responsive Fluorescence Switching: The Reversible Piezochromism and Protonation Effect of a Divinylanthracene Derivative. *J. Mater. Chem. C* **2013**, *1* (45), 7554. https://doi.org/10.1039/c3tc31553c.

(5) Zhang, Y.; Qile, M.; Sun, J.; Xu, M.; Wang, K.; Cao, F.; Li, W.; Song, Q.; Zou, B.; Zhang, C. Ratiometric Pressure Sensors Based on Cyano-Substituted Oligo(p-Phenylene Vinylene) Derivatives in the Hybridized Local and Charge-Transfer Excited State. *J. Mater. Chem. C* **2016**, *4* (42), 9954–9960. https://doi.org/10.1039/C6TC03157A.

(6) Zhou, H.; Yang, L.; You, W. Rational Design of High Performance Conjugated Polymers for Organic Solar Cells. *Macromolecules* **2012**, *45* (2), 607–632. https://doi.org/10.1021/ma201648t.

(7) Li, H.; Han, J.; Zhao, H.; Liu, X.; Luo, Y.; Shi, Y.; Liu, C.; Jin, M.; Ding, D. Lighting Up the Invisible Twisted Intramolecular Charge Transfer State by High Pressure. *J. Phys. Chem. Lett.* **2019**, *10* (4), 748–753. https://doi.org/10.1021/acs.jpclett.9b00026.

(8) Wu, J.; Wang, W.; Gong, C.; Li, Q.; Li, Z.; Deng, G.; Zhang, X.; Chen, K.; Gong, Y.; Chiang, K. S. Tuning the Strength of Intramolecular Charge-Transfer of Triene-Based Nonlinear Optical Dyes for Electro-Optics and Optofluidic Lasers. *J. Mater. Chem. C* **2017**, *5* (30), 7472–7478. https://doi.org/10.1039/C7TC00958E.

(9) Hoffmann, R.; Imamura, A.; Zeiss, G. D. Spirarenes. *J. Am. Chem. Soc.* **1967**, *89* (20), 5215–5220. https://doi.org/10.1021/ja00996a023.

(10) Simmons, H. E.; Fukunaga, T. Spiroconjugation. *J. Am. Chem. Soc.* **1967**, *89* (20), 5208–5215. https://doi.org/10.1021/ja00996a022.

(11) Schweig, A.; Weidner, U.; Hellwinkel, D.; Krapp, W. Spiroconjugation. *Angew. Chem. Int. Ed.* **1973**, *12* (4), 310–311. https://doi.org/10.1002/anie.197303101.

(12) Dürr, H.; Gleiter, R. Spiroconjugation. *Angew. Chem. Int. Ed.* **1978**, *17* (8), 559–569. https://doi.org/10.1002/anie.197805591.

(13) Schönberg, A.; Singer, E.; Stephan, W.; Sheldrick, W. S. Extremely Reactive Carbon-Carbon Double Bonds-I. *Tetrahedron* **1983**, *39* (14), 2429–2437. https://doi.org/10.1016/S0040-4020(01)91970-2.

(14) Sohönberg, A.; Singer, E.; Osch, M.; Hoyer, G.-A. 1,2,3-Tricarbonylverbindungen, XI. *Tetrahedron Lett.* **1975**, *16* (37), 3217–3220. https://doi.org/10.1016/S0040-4039(00)91460-6.

(15) Schönberg, A.; Singer, E. Die Chemie Des Ninhydrins Und Anderer Cyclischer 1,2,3-Tricarbonylverbindungen. *Tetrahedron* **1978**, *34* (9), 1283. https://doi.org/10.1016/0040-4020(78)88321-5.

(16) Schönberg, A.; Singer, E.; Eckert, P. 1,2,3-Tricarbonylverbindungen, XIV. Über Die Photochemische Epoxidierung Einer Carbonylgruppe Mit Methanol. *Chem. Ber.* **1980**, *113* (9), 3094–3097. https://doi.org/10.1002/cber.19801130925.

(17) Maslak, P.; Chopra, A. Spiroconjugated Intramolecular Charge-Transfer Dyes. *J. Am. Chem. Soc.* **1993**, *115* (20), 9331–9332. https://doi.org/10.1021/ja00073a076.

(18) Maslak, P. Spiroconjugation: An Added Dimensi in the Design of Organic Molecular Materials. *Adv. Mater.* **1994**, *6* (5), 405–407. https://doi.org/10.1002/adma.19940060515.

(19) Maslak, P.; Augustine, M. P.; Burkey, J. D. Toward Molecular Charge-Transfer Relays. A Three-Dimensional Acceptor and Its Radical Anion. *J. Am. Chem. Soc.* **1990**, *112* (13), 5359–5360. https://doi.org/10.1021/ja00169a058.

(20) Maslak, P.; Chopra, A.; Moylan, C. R.; Wortmann, R.; Lebus, S.; Rheingold, A. L.; Yap, G. P. A. Optical Properties of Spiroconjugated Charge-Transfer Dyes. *J. Am. Chem. Soc.* **1996**, *118* (6), 1471–1481. https://doi.org/10.1021/ja9533003.

(21) Gleiter, R.; Hoffmann, H.; Irngartinger, H.; Nixdorf, M. Donor-Acceptor Spiro-Compounds — Syntheses, Structures, and Electronic Properties. *Chem. Ber.* **1994**, *127* (11), 2215–2224. https://doi.org/10.1002/cber.1491271121.

(22) Wilbuer, J.; Schnakenburg, G.; Esser, B. Syntheses, Structures and Optoelectronic Properties of Spiroconjugated Cyclic Ketones. *Eur. J. Org. Chem.* **2016**, *2016* (14), 2404–2412. https://doi.org/10.1002/ejoc.201600235.

(23) Wössner, J. S.; Grenz, D. C.; Kratzert, D.; Esser, B. Tuning the Optical Properties of Spiro-Centered Charge-Transfer Dyes by Extending the Donor or Acceptor Part. *Org. Chem. Front.* **2019**, *6*, 3649–3656. https://doi.org/10.1039/C9QO01134J.

(24) Luo, L.; Meng, L.; Sun, Q.; Ge, Z.; Li, R. Novel Synthesis of Thiazolo/Thienoazepine-5,8-Diones from Dihalo Cyclic 1,3-Diketones and Mercaptonitrile Salts. *RSC Adv.* **2014**, *4* (13), 6845–6849. https://doi.org/10.1039/C3RA46606J.

(25) Li, R.; Liu, G.; Xiao, M.; Yang, X.; Liu, X.; Wang, Z.; Ying, L.; Huang, F.; Cao, Y. Non-Fullerene Acceptors Based on Fused-Ring Oligomers for Efficient Polymer Solar Cells via Complementary Light-Absorption. *J. Mater. Chem. A* **2017**, *5* (45), 23926–23936. https://doi.org/10.1039/C7TA06631G.

(26) Gleiter, R.; Haberhauer, G.; Werz, D. B.; Rominger, F.; Bleiholder, C. From Noncovalent Chalcogen–Chalcogen Interactions to Supramolecular Aggregates: Experiments and Calculations. *Chem. Rev.* **2018**, *118* (4), 2010–2041. https://doi.org/10.1021/acs.chemrev.7b00449.

(27) D'Andrade, B. W.; Datta, S.; Forrest, S. R.; Djurovich, P.; Polikarpov, E.; Thompson, M. E. Relationship between the Ionization and Oxidation Potentials of Molecular Organic Semiconductors. *Org. Electron.* **2005**, *6* (1), 11–20. https://doi.org/10.1016/j.orgel.2005.01.002.

(28) Zelle, R. E.; McClellan, W. J. A Simple, High-Yielding Method for the Methylenation of Catechols. *Tetrahedron Lett.* **1991**, *32* (22), 2461–2464. https://doi.org/10.1016/S0040-4039(00)74353-X.

(29) Becke, A. D. Density-functional Thermochemistry. III. The Role of Exact Exchange. *J. Chem. Phys.* **1993**, *98* (7), 5648–5652. https://doi.org/10.1063/1.464913.

(30) Grimme, S.; Antony, J.; Ehrlich, S.; Krieg, H. A Consistent and Accurate Ab Initio Parametrization of Density Functional Dispersion Correction (DFT-D) for the 94 Elements H-Pu. *J. Chem. Phys.* **2010**, *132* (15), 154104. https://doi.org/10.1063/1.3382344.

(31) Schäfer, A.; Huber, C.; Ahlrichs, R. Fully Optimized Contracted Gaussian Basis Sets of Triple Zeta Valence Quality for Atoms Li to Kr. *J. Chem. Phys.* **1994**, *100* (8), 5829–5835. https://doi.org/10.1063/1.467146.

(32) TURBOMOLE V7.3 2018, a development of University of Karlsruhe and Forschungszentrum Karlsruhe GmbH, 1989-2007, TURBOMOLE GmbH, since 2007; available from http://www.turbomole.com.

(33) Tom, C. T. M. B.; Crellin, J. E.; Motiwala, H. F.; Stone, M. B.; Davda, D.; Walker, W.; Kuo, Y.-H.; Hernandez, J. L.; Labby, K. J.; Gomez-Rodriguez, L.; et al. Chemoselective Ratiometric Imaging of Protein S-Sulfenylation. *Chem. Commun.* **2017**, *53* (53), 7385–7388. https://doi.org/10.1039/C7CC02285A.

Table of Contents graphic